

Processes Determining The Dimensional Change Of PM Steels

F. J. Semel
Hoeganaes Corporation, Cinnaminson, NJ 08077

Presented at PM²TEC2001
International Conference on Powder Metallurgy & Particulate Materials
May 13 – 17, 2001, New Orleans, Louisiana.

ABSTRACT

The dimensional change characteristics of PM steels are generally not determined by the effects of the processes that occur at the sintering temperature. Instead, dilatometry shows that the largest contributions are typically due to the combined effects of various lower temperature processes. The present report both illustrates and discusses these effects in various common PM steels.

INTRODUCTION

Given the emphasis on time and temperature in discussions of sintering, it is perhaps natural to conclude that the dimensional change during the process is mainly, if not entirely, a consequence of the processes that occur at the sintering temperature. Thus, the common view is that this important parameter is largely dependent upon and will therefore be responsive to the so-called sintering conditions which in addition to the sintering time and temperature are normally considered to include the sintering atmosphere as well. In fact, numerous dilatometric studies in these laboratories over the years have shown that while these conditions are important, they generally account for less than half and frequently less than a third of the dimensional change that is observed in the most common P/M compositions. Indeed, the balance of the dimensional change and often the greatest part of it is determined by various processes and effects that occur during the heating and cooling stages of the process. These include the behavior of the lubricant as it effects the early thermal expansion of the compact and the amount of low temperature sintering that occurs as well as contributions associated with the heating and cooling transformation behaviors and the thermal expansion and contraction characteristics which otherwise typify the process.

The purpose of this report is to present the results of dilatometric studies which show these effects in the sintering of the eutectoid iron-carbon and iron-carbon-copper systems, namely, F-0008 and FC-0208 respectively.

EXPERIMENTAL PROCEDURE

The experimental procedure consisted in conducting a series of dilatometric sintering trials that started with an essentially pure grade of iron powder and progressed in compositional increments to an FC-0208 composition of the same grade of iron powder. Thus, the series included iron, iron plus lubricant, iron plus graphite, iron plus lubricant plus graphite and lastly, iron plus lubricant plus graphite plus copper. Re-sintering trials of several of these combinations were also conducted to provide direct comparisons between the dilatometric records of the specimen in the as-sintered and re-sintered states.

The iron powder used in the study was Hoeganaes Ancorsteel 1000B. The lubricant was Lonza Acrawax C. For the powders that were compacted without benefit of an admixed lubricant, the Acrawax was suspended in alcohol and provided as a die wall lubricant. For the powders that contained it as an admixed addition, the Acrawax was added in the amount of 0.75% by weight. The graphite used in the study was a screened grade of Asbury 3031 and in the compositions in which it appears it was added in the amount of 0.85% by weight. The copper powder used was AcuPowder 8081 and in the single composition in which it appears it was added in the amount of 2% by weight. The admixtures in each case were regular mixes and were prepared by bottle mixing.

The sintering trials were conducted in an horizontal dilatometer as designed and built by Harpor Industries, Inc. A schematic of the unit is shown below in Figure 1.

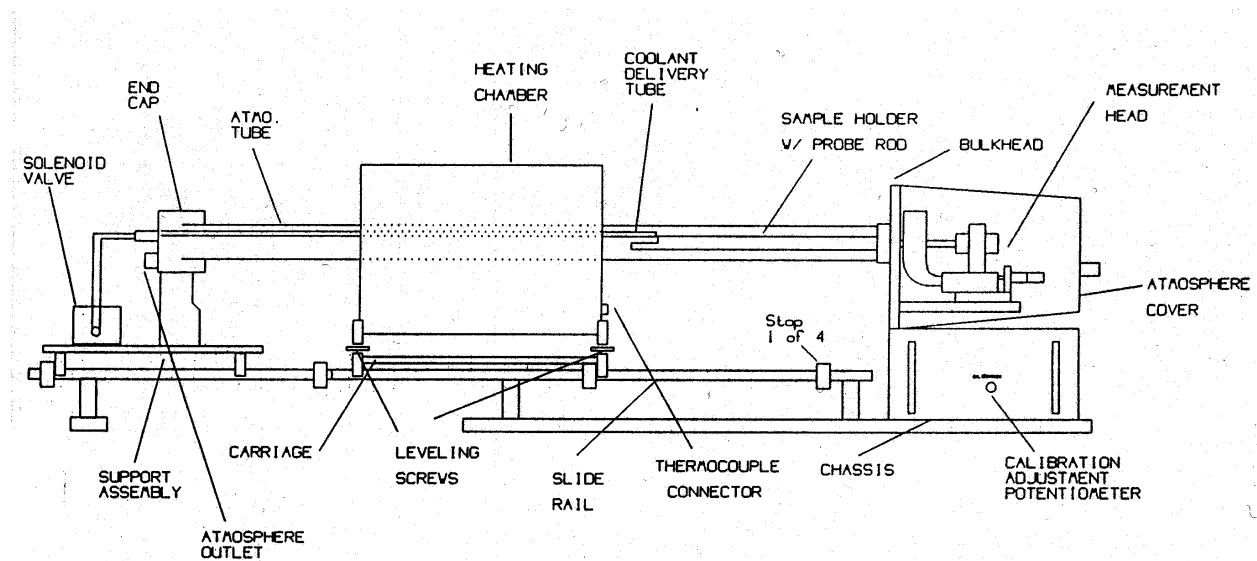


Figure 1 - Schematic Of Harpor TD-720 Series Dilatometer.

In addition to the features indicated in the figure, the unit accommodates a standard Charpy impact specimen, (ASTM E 23), and is otherwise equipped with a constant force measuring head and a West 4400 programmable controller. Time, temperature and dilation data are acquired electronically and stored digitally. The data are analyzed subsequent to acquisition in a Microsoft Excel environment using a program that was developed in this laboratory. The impact specimens used in the study were compacted to a standard height and density of 1.1 cm and 7.0 g/cm^3 and were otherwise prepared with a thermocouple well at one end which

measured 1.6 mm in diameter and 7 mm in depth. The constant force of the measuring head on the specimen during sintering corresponded to a pressure of just upwards of 0.1 atmosphere, (1.5 psi). Micrometer and weight measurements to estimate the green and sintered densities of the specimens, (ASTM B331), as well as to provide a check on the final dilatometric indication were also conducted.

A standard sintering practice was employed as follows. The dilatometer furnace was heated with the specimen in place at a rate of 10 °C/min. to 1100 °C and then at a rate of 5 °C/min. to 1120 °C, (2050 °F), and held at temperature for 30 minutes. Initial cooling was at a rate of 10 °C/min. to 850 °C, (1560 °F), followed by natural furnace cooling to room temperature. The atmosphere was a mixture of 6% hydrogen by volume in helium at a flowrate of 0.085 m³/hr., (i.e. 3 cfh). Both gases were ultra high purity grades with nominal dew points of -20 °C, (0 °F), or better.

RESULTS AND DISCUSSION

It may be useful to begin by pointing out that solid state sintering may occur by any one of four mechanisms and in the general case is a cumulative effect of all four. These include the vapor transport and the surface, volume, and grain boundary diffusion mechanisms, (1). The vapor transport and surface diffusion mechanisms effect metallurgical bonding and pore rounding but cause no densification. Thus, the occurrence of these mechanisms is not detectable by dilatometry. In contrast, in addition to bonding and pore rounding, the volume and grain boundary mechanisms also effect pore elimination and hence, densification. Thus, the occurrence of these mechanisms is detectable by dilatometry. Moreover, since these mechanisms tend to be dominant in different temperature regimes, dilatometry may also provide a clue as to their relative contributions. However, in the general case, it will be appreciated that in view of the existence of sintering mechanisms that cause densification and mechanisms that don't, the lack of a dilatometric change that's attributable to sintering does not imply the absence of sintering. On the other hand, as will be seen, there are also mechanisms other than sintering that can cause dilatometric change and in some cases densification.

Sintering Of A Plain Iron Powder.

The dilatometric results of the sintering a plain iron powder specimen as compacted in the die wall lubricated condition are shown below in Figure 2 and Table 1. The data in the table serve to quantify the dilatometric indications of the figure. In particular, in addition to the high temperature and as-sintered dimensional change values that are indicated in the figure, the table also lists the coefficients of thermal expansion and contraction for selected temperature intervals in both the α and γ stability ranges as well as the corresponding α / γ transformation temperatures and dilations that were observed. As will be explained, various thermal and transformation effects contributed as much to the overall dimensional change in this case as did sintering and the latter data are useful to analyze these effects.

Both the dilatometric indications in Figure 2 and the dimensional change data in the accompanying table show that in spite of the fact that there was very little shrinkage at the sintering temperature, the overall change from green was nevertheless slightly in excess of -104 ums absolute or -0.19% relative to the original length L_0 , (i.e. 54,250 ums or ~ 2.13 ins).

Sintering of a Plain Iron Powder Compact

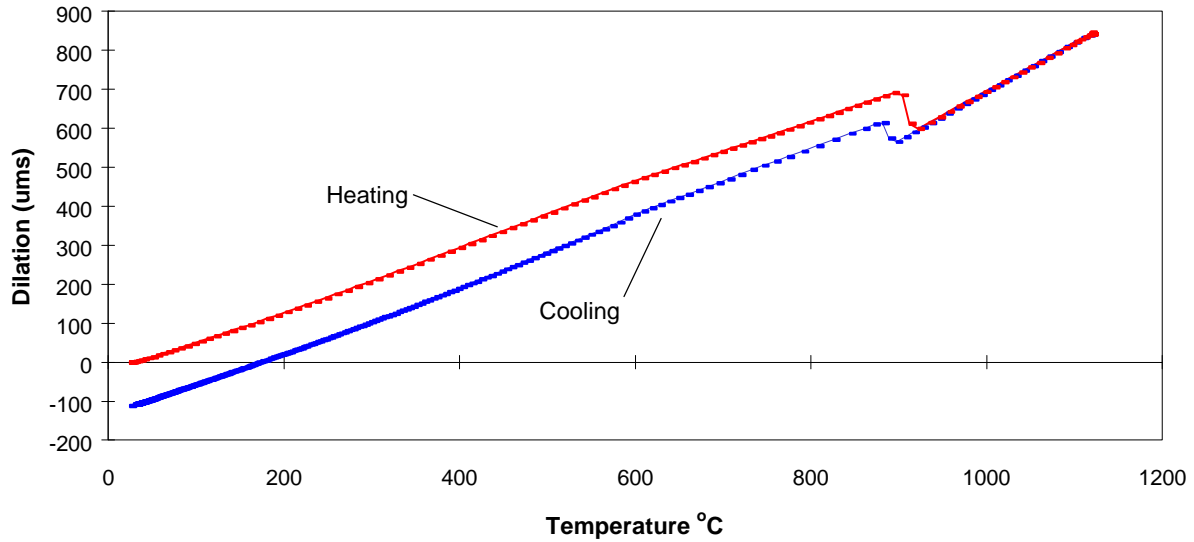


Figure 2 - Dilation vs. Temperature During Sintering Of A Plain Iron Powder Compact.

Table 1 - Dilatometric Indications Of The Sintering Of A Plain Iron Power Compact.

Dimensional Change Data		
Condition	ΔL (ums)	$\Delta L/L_o$ %
At 1120 °C	-3.4	-0.006
As-Sintered	-104.7	-0.193
Thermal Data		
Temperature Range °C	Coefficient of Expansion cm/cm/°C	Coefficient of Contraction cm/cm/°C
200 - 400 (α -phase)	1.54E-05	1.55E-05
500 - 700 (α -phase)	1.48E-05	1.68E-05
900 - 1100 (γ -phase)	2.33E-05	2.33E-05
Transformation Data		
Property	α to γ	γ to α
Start Temperature - °C	900	892
Finish Temperature - °C	915	881
Dilation - (ums)	-104	+59
Dimensional Change Analysis		
Origin of Contribution	ΔL (ums)	$\Delta L/L_o$ %
Thermal Effects	-13.8	-0.026
Net Transformation Dilation	-45.0	-0.083
Latent Process Effects	-42.5	-0.078

Reference to the figure will show that most of this change occurred in the alpha stability range and was at least partially connected with differences in the dilations that accompanied the phase changes. According to the data in the table, the transformation dilations on heating and cooling were -104 μm and +59 μm respectively for a net transformation dilation of -45.0 μm absolute or -0.083%. In addition, although not as obvious as the foregoing, there was also a thermal effect due to the differences in the expansion/contraction coefficients of the two phases and the temperatures at which the phase changes occurred on heating and cooling. Accordingly, a further review of Figure 2 will show that the phase change occurred at a lower temperature on cooling than it did on heating and that as a result of the differences in the slopes of the curves in the two stability ranges which, of course, reflect the near thermal coefficients of the phases, there was some additional shrinkage of the specimen during the change. Its magnitude may be estimated from the differences in the transformation temperatures, the corresponding thermal coefficients of the phases and the original length of the specimen, L_0 . According to the data in Table 2, its value in this case was -13.8 μm absolute or -0.026%.

The combined result of these two effects plus the indicated sintering effect at 1120 $^{\circ}\text{C}$ is -62.2 μm leaving an unexplained absolute balance of -42.5 μm or -0.078%. This is indicated in Table 1 as a so-called latent process effect. Such effects are normally due to sintering but necessarily include experimental error as well. In this case, if it is assumed to be a sintering effect then since it evidently did not occur at the sintering temperature, its necessary to speculate that it occurred mostly during heating and possibly, to a lesser extent, during cooling as well. One way to confirm this speculation is to re-sinter the specimen and compare its dilatometric behavior to that in the as-sintered state. If the indicated sintering effect exists then there should be telltale differences in the two behaviors. Significantly, the difference in the values of the α phase coefficients of expansion and contraction that are indicated in Table 1 in the 500 to 700 $^{\circ}\text{C}$ range provide an important clue as to where to look to for these differences.

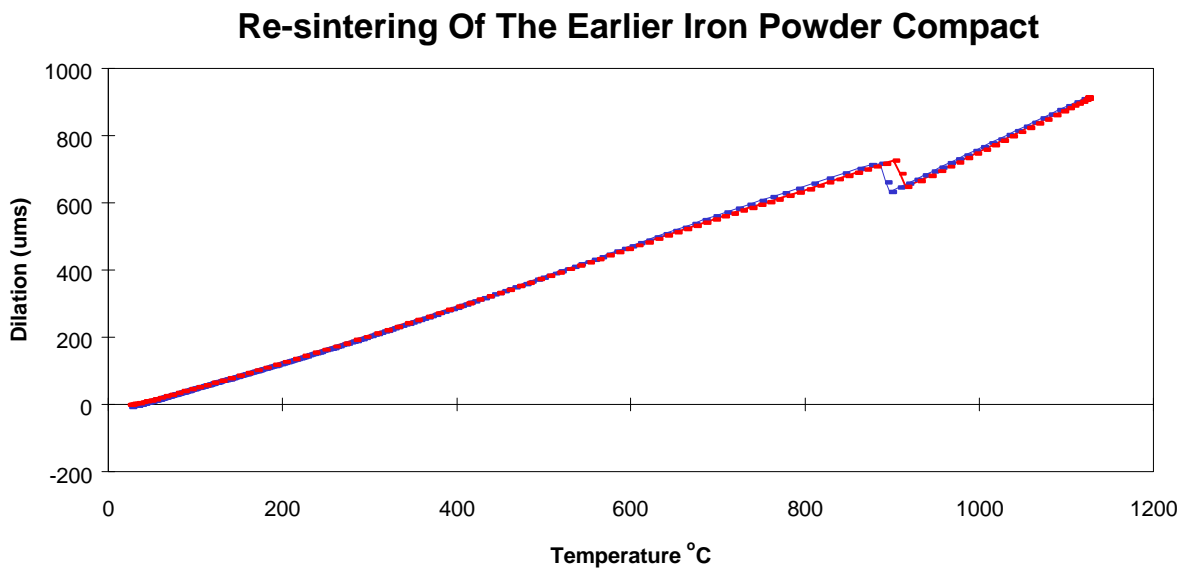


Figure 3 - Dilation vs. Temperature During Re-sintering Of The Earlier Iron Powder Compact.

The dilatometric record of the re-sintered specimen is shown in Figure 3. As will be evident from a review of the figure, there was very little change in the length of the specimen in this case. In actual fact, the hard data indicated a small net growth of about 10 μm s which was mostly attributable to the differences in the transformation dilations that are evident in the figure. Notice, in particular, that this behavior is different in both magnitude and sense than the earlier behavior in which, of course, the transformation dilations effected a net shrinkage that was roughly five times as large as the present one. The important point being that the net effect of the phase transformations may be positive or negative and is largely unpredictable and therefore, uncontrollable.

In any event, the findings in the present case also showed two other important differences in comparison with the earlier findings. First, as is evident by inspection of Figure 3, the heating and cooling curves in this case are virtually identical to each other whereas the previously mentioned differences in the thermal coefficients in the 500 to 700 $^{\circ}\text{C}$ range clearly show that this was not true in the earlier case. Second, actual determination of the thermal coefficients in this case showed that they were essentially the same as in the earlier case except in the 500 to 700 $^{\circ}\text{C}$ range. The latter value was $1.61\text{E-}05 \text{ cm/cm}^{\circ}\text{C}$, the same during both expansion and contraction. Comparison of this value with the values presented in Table 1 will show that it is intermediate the two but closer in magnitude to the contraction value. The implication is that the observed sintering in the earlier case occurred entirely in the α phase stability range and mostly during heating at temperatures above 500 $^{\circ}\text{C}$. Thus, comparison of the α phase expansion records of the specimen in the as-sintered and re-sintered states should provide direct evidence of this. This comparison is shown below in Figure 4.

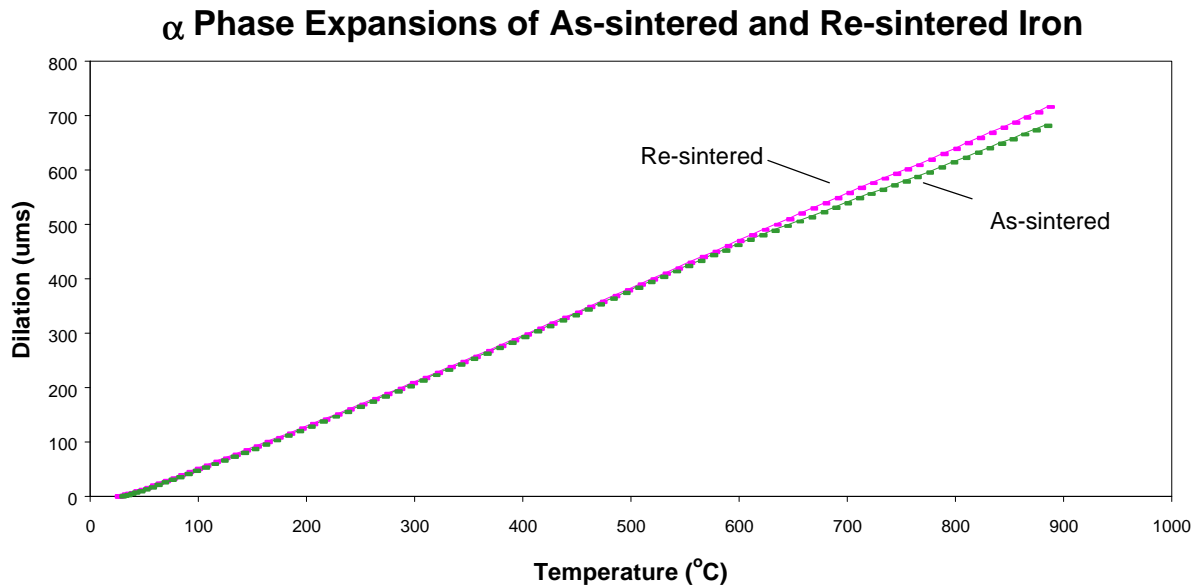


Figure 4 - α Phase Dilations vs Temperature of an Iron Powder Compact in the As-sintered and Re-sintered Conditions.

As a casual inspection of this figure will show, the deviation in the heating curves with increasing temperature confirms the existence of the indicated sintering effect. Quantitatively, the magnitude of the difference indicated by the hard data just prior to the α to γ transformation

turned out to be -30.5 μm s and explains roughly 72% of the latent process effect that was indicated in Table 1. The balance of 12 μm s is thought to be attributable to α phase sintering during cooling and experimental error.

The reason, of course, for the greater sintering in the α phase than at the higher temperatures in the γ phase is that the iron generally diffuses faster in the α than it does in the γ . For example, the bulk diffusivity at 850 $^{\circ}\text{C}$ in the α is roughly equal to what it is in the γ at the sintering temperature, (2). In addition, the α phase would be expected to support a higher dislocation density than the γ at virtually all temperatures, especially just subsequent to compaction during the heating step and consequently, provide greater sintering as a result of various thermally activated dislocation processes, (3).

Sintering Of Iron Powder Plus Lubricant.

The dilatometric results of sintering a compact of the same grade iron powder but with admixed lubricant are shown below in Figure 5 and Table 2. Here again, the data in the table serve to quantify the dilatometric indications of the figure.

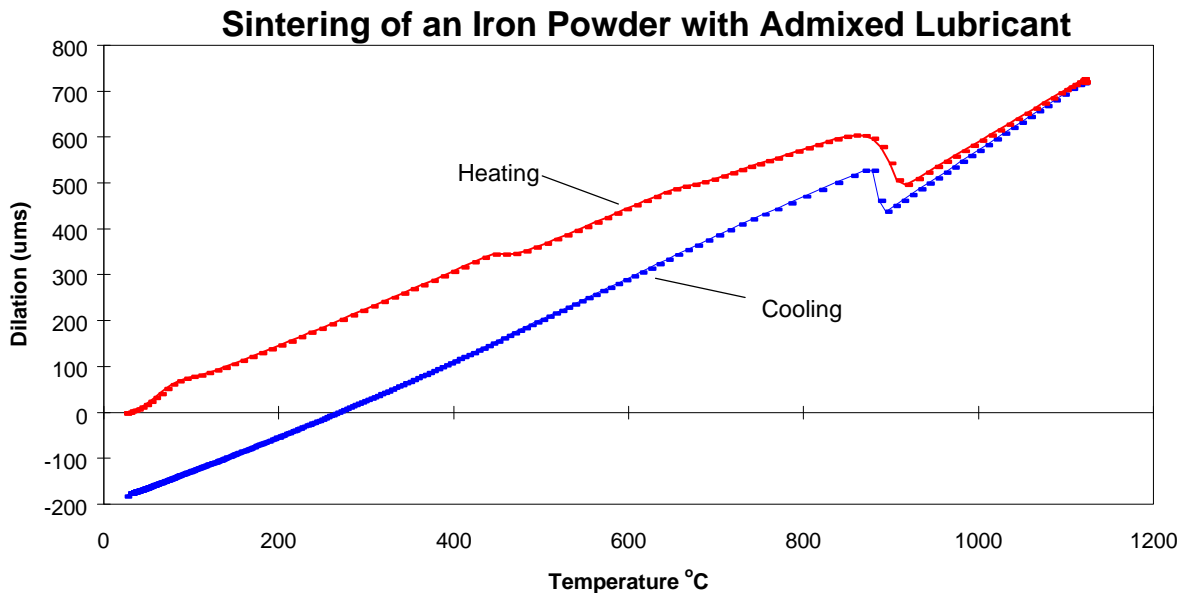


Figure 5 - Dilatation vs Temperature During Sintering of an Iron Powder Compact With Admixed Lubricant.

As will be evident from the figure, there were both similarities and differences in the behavior of this specimen in comparison with that of the plain iron specimen. Perhaps the two most obvious differences include the rapid early expansion and the later break in the upward trend of the heating curve just above 400 $^{\circ}\text{C}$. Both effects are traceable to the presence of the admixed lubricant and, as a matter of interest, are not necessarily peculiar to this particular lubricant since somewhat similar effects are seen with other lubricants as well. The cause of the low temperature expansion is unknown. Limited studies of the effect have shown that it is not due either to a glass transition or to melting of the lubricant because it occurs both with lubricants that do and do not exhibit a glass transition, (e.g. zinc stearate), and typically peaks at temperatures that are substantially below the melting point. The break in the curve at the

higher temperature, on the other hand, correlates with lubricant burn-off which in the case of Acrawax has been shown by thermogravimetric analysis to occur at about 450 °C, (4).

Another obvious difference in the behavior of this specimen in comparison with that of the plain iron specimen and one which, in fact, is rarely seen, is the disparity in the slopes of the heating and cooling curves in the γ phase stability range, (i.e. above 910 °C). The cause is uncertain so it was regarded as a thermal effect. However, it may in fact be due to sintering by the grain boundary diffusion mechanism during the heating step. In any case, the cumulative contribution to the final dimensional change of the specimen was estimated to be -30.7 ums absolute or -0.057%.

Table 2 - Dilatometric Indications Of The Sintering Of An Iron Power Compact With Admixed Lubricant

Dimensional Change Data		
Condition	ΔL (ums)	$\Delta L/L_0$ %
At 1120 °C	-7.9	-0.015
As-Sintered	-177.8	-0.328
Thermal Data		
Temperature Range °C	Coefficient of Expansion cm/cm/°C	Coefficient of Contraction cm/cm/°C
200 - 400 (α -phase)	1.50E-05	1.51E-05
500 - 700 (α -phase)	1.34E-05	1.68E-05
900 - 1100 (γ -phase)	2.10E-05	2.32E-05
Transformation Data		
Property	α to γ	γ to α
Start Temperature - °C	867	890
Finish Temperature - °C	912	877
Dilation - (ums)	-112	102
Dimensional Change Analysis		
Origin of Contribution	ΔL (ums)	$\Delta L/L_0$ %
Thermal Effects	-65.6	-0.121
Net Transformation Dilation	-10.0	-0.018
Latent Process Effects	-94.3	-0.174

The tabulated data in Table 2 showed an important similarity and yet another interesting difference in the behavior of this specimen versus the earlier one. The similarity was in the magnitudes of the thermal coefficients in the 500 to 700 °C range. Here again, the observed values bracketed the expected value, (i.e. ~1.6E-05), and thus indicated the likelihood of α phase sintering as a primary contributor to the final dimensional change value. The difference mentioned was in the α to γ transformation temperatures. The plain iron powder specimen transformed in the range of 905 to 915 °C, precisely the temperatures that would be expected of a commercially pure iron. In contrast, the present specimen transformed in the range of 867 to 912 °C; the lower start temperature being a clear-cut indication of a higher carbon content and thus an indication of either graphite contamination of the starting materials or carbon

pickup from the decomposition of the lubricant. Subsequent chemical analysis confirmed the presence of the suspected higher carbon. Its value was 0.014% versus 0.005% for the plain iron specimen. Reference to an iron-carbon phase diagram will confirm that this difference is more than adequate to cause the observed differences in the transformation start temperatures, (5). A separate study as to the origin of the carbon strongly suggested that it was probably due to lubricant decomposition rather than to graphite contamination.

The dimensional change analysis that is presented in Table 2 indicated that the latent process effect was by far the major contributor to the final dimensional change value that was observed in this case. According to the breakdown in the table, the thermal and transformation effects only accounted for about 43% of the change. Of the balance, -7.9 μm s or a little less than 5% of the total change was attributable to sintering in the γ stability range at 1120 °C. The remaining -94.3 μm s or what amounts to upwards of 50% of the total change was apparently again due to sintering that occurred in the α stability range.

As previously, in order to confirm this speculation, the specimen was re-sintered so that its dilatometric behavior could be compared with that in the as-sintered state. As it turned out, its behavior during re-sintering was very similar to that of the re-sintered plain iron specimen as earlier shown in Figure 3 and needn't be further reviewed or discussed. The comparison to the as-sintered condition is shown below in Figure 6.

α Phase Expansions of As-sintered and Re-sintered Iron with Admixed Lubricant

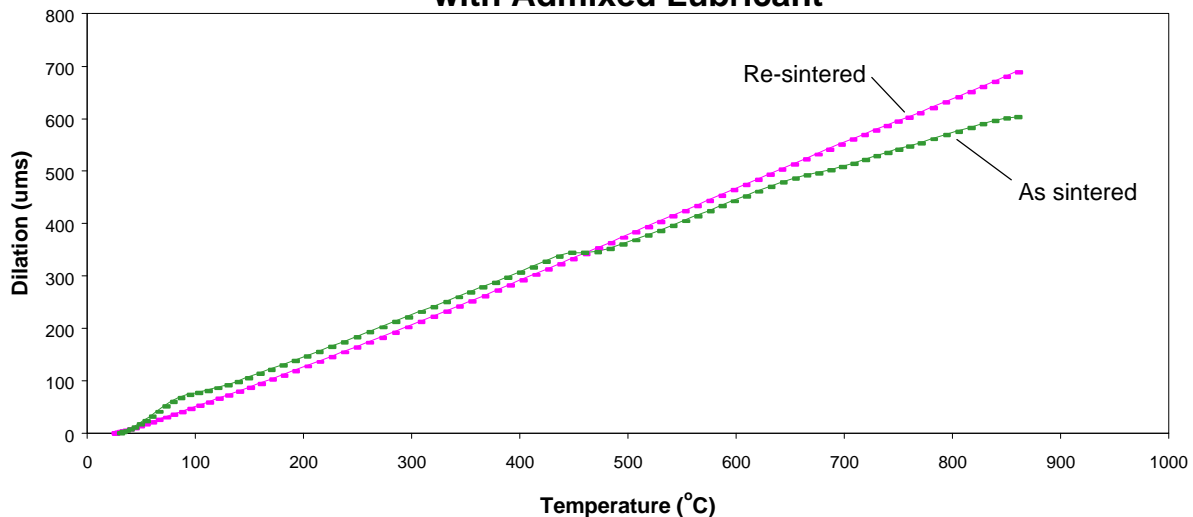


Figure 6 - α Phase Dilations vs. Temperature of an Iron Powder Compact With Admixed Lubricant in the As-sintered and Re-sintered Conditions.

The as-sintered curve here is shown up to the transformation start temperature. Thus, the magnitude of the α phase sintering that is indicated as having occurred during the heating step is -85.8 μm s which explains a little over 90% of the earlier mentioned value of -91.7 μm s. As in the case of the plain iron specimen, the difference which amounts to roughly -6 μm s is thought to be attributable to α phase sintering during cooling and experimental error. In addition, notice

that this comparison also shows that the early expansion due to the initial presence of the lubricant was later offset by a contraction that accompanied its decomposition.

Finally, as may already be evident, a comparison of the present figure with the earlier Figure 4 will show that the α phase sintering contribution in this case was substantially greater than in the plain iron specimen. Apparently, the lubricant has an activating effect. However, the mechanism is unknown. Limited studies indicated that it is evidently not a result of early oxide reduction due to the hydrocarbons that are present in the lubricant's chemical makeup. For example, to determine the effect of early reduction, a plain iron specimen was sintered in pure hydrogen using a reduced heating rate of 5 °C/min up to 500 °C. Thereafter, the heating rate was increased to 10 °C/min. Although this practice resulted in a modest improvement in the amount of α phase sintering that was observed in comparison with the plain iron specimen of Figure 4, the magnitude of the improvement was no where near as great as the one that was observed with the present specimen.

Sintering Of Iron Powder Plus Graphite.

The dilatometric results of sintering a compact of the same grade iron powder but now with admixed graphite are shown below in Figure 7 and Table 3. As in the case of the plain iron specimen, die wall lubrication was used to facilitate the compaction step.

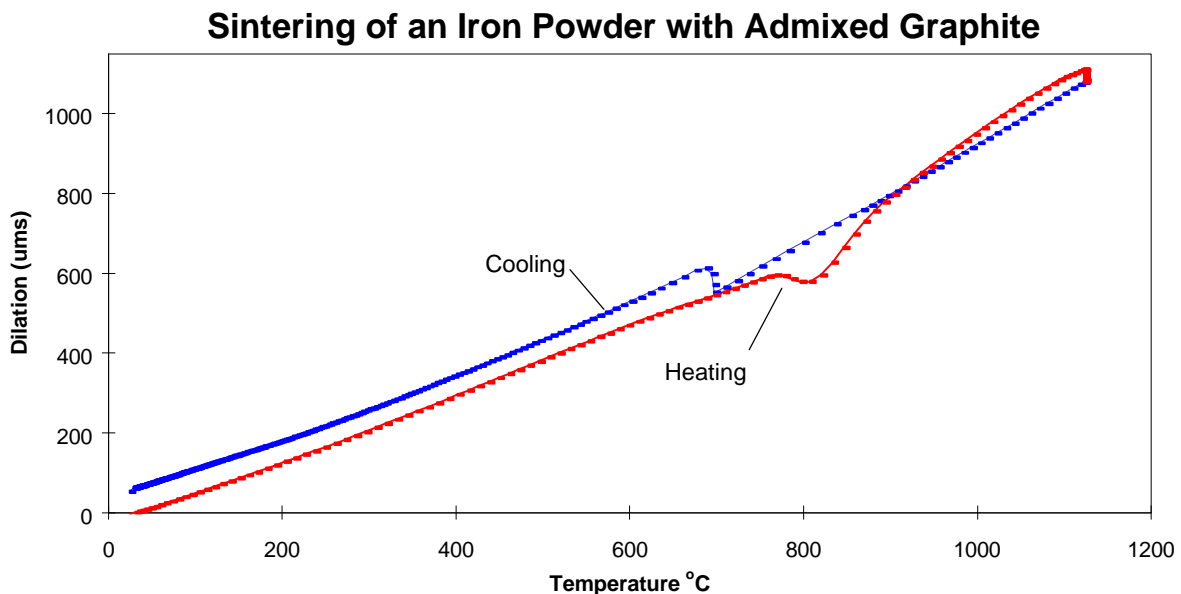


Figure 7 - Dilatation vs. Temperature During Sintering of an Iron Powder Compact With Admixed Graphite.

As will be evident from a comparison of this figure with the earlier Figure 2, there were several significant differences in the behavior of the specimen in comparison with that of the plain iron specimen. The most obvious difference, of course, is that the cooling curve in this case intersects the heating curve at a relatively high temperature and thereafter continues to descend well above it. Thus, the overall result of the process was one of net growth rather than shrinkage as in the earlier case. Other obvious differences include both the manner of the α to γ transformation and the way the specimen subsequently expanded in the γ stability range

as well as the amount of shrinkage that occurred at the sintering temperature. There was also a significant difference in the temperatures at which the γ phase transformed back to the α during cooling but this is perhaps not as obvious by inspection of the two figures as the latter differences. A direct comparison of the tabulated data in the two cases, however, will clearly show it.

Table 3 - Dilatometric Indications Of The Sintering Of An Iron Power Compact With Admixed Graphite.

Dimensional Change Data		
Condition	ΔL (μms)	$\Delta L/L_0$ %
At 1120 °C	-41.6	-0.077
As-Sintered	+ 63.2	+0.117
Thermal Data		
Temperature Range °C	Coefficient of Expansion cm/cm/°C	Coefficient of Contraction cm/cm/°C
200 - 400 (α -phase)	1.56E-05	1.52E-05
450 - 650 (α -phase)	1.59E-05	1.57E-05
900 - 1100 (γ -phase)	- - -	2.33E-05
Transformation Data		
Property	α to γ	γ to α
Start Temperature - °C	771	696
Finish Temperature - °C	803	684
Dilation - (μms)	-18.0	64.6
Dimensional Change Analysis		
Origin of Contribution	ΔL (μms)	$\Delta L/L_0$ %
Graphite Solution	+135.1	+0.249
Thermal Effects	-60.2	-0.111
Net Transformation Dilation	+46.6	+0.086
Latent Process Effects	-16.7	-0.031

The observed growth in this case is mostly, if not entirely, the result of the presence of the admixed graphite and its effects on the specimen's behavior during the α to γ transformation and subsequently during heating in the γ range.

The transformation effects are especially complex. Compared to a plain iron specimen, the transformation of a graphite containing specimen will generally start at a lower temperature, occur over a much larger temperature range and produce a smaller transformation dilation. Reference to an Fe-C phase diagram will show that the lowest possible start temperature is 735 °C. However, while the transformation of an iron-graphite compact may actually begin at this low a temperature, its start will not be detectable by dilatometry until a somewhat higher temperature. The reason is that there are several conflicting processes that determine the specimen's dimensions and the observable dilation reflects the occurrence of all of them rather than any one. For example, as the temperature of the specimen exceeds the minimum graphite solution temperature, these include in order of increasing importance: 1) sintering; 2) thermal expansion; 3) graphite solution; 4) transformation; and, 5) the response of the

specimen to the stress state that arises in consequence of the thermal gradients that are present.

The effects of the first two of these processes are generally well known. In the case of the last three, the individual effects are as follows. As the graphite goes into solution, it displaces its own volume in the iron and produces a growth effect. At the same time, it also causes the iron to transform from the α phase to the denser γ and conversely produces a much larger shrinkage effect. And finally, since the contribution of each of the four processes involved is temperature dependent, the natural presence of thermal gradients in the specimen produces a complex state of stress that may have significant adverse effects overall. In particular, depending on how much bonding occurred prior to the onset of transformation, the stresses may actually be large enough to break pre-existing sinter bonds and reverse much, if not all, of the prior densification even including some that occurred in the compaction step.

Experience has shown that while the magnitude of the latter effect is not quantifiable, it normally correlates with higher apparent start temperatures and smaller net dilations. According to the data in Table 3, the transformation in the present case started at a temperature of 771 °C which is relatively high and was accompanied by a dilation of -18 ums absolute or -0.033% which is correspondingly, rather small. Thus, the implication is that the pre-existing sinter bonds of this specimen were not strong enough to survive the stresses that arose during the phase change and it consequently lost density in the process. As will be shown later, there is reason to believe that the purported weak sinter bonds here were in fact an adverse effect of the admixed graphite on the α phase sintering that occurred.

As a general matter, any graphite that remains after the transformation now goes into solution and with continued heating, the growth effects that were previously mentioned as attending its dissolution affect the shape of the heating curve. The heating curve subsequent to transformation that is shown by the dilatometric record of the present specimen is typical of such effects. Since the heating curve in the absence of the graphite would be a straight line that roughly parallels the straight line of the cooling curve, it is possible to estimate the associated growth effect. The value in the present case is listed in the tabulated data as part of the dimensional change analysis under the heading of graphite solution effects. Notice that it is by far the largest growth effect listed.

Notably, the sintering effect at 1120 °C that was shown by the dilatometric record in this case was substantially larger than the sintering effects that were seen in the records of the earlier specimens. Interestingly, this too is almost certainly an effect of the graphite since the presence of dissolved carbon in the iron increases its diffusivity. For example, the diffusivity of iron with 0.75% carbon at 1120 °C is roughly five times that of pure iron at the same temperature, (6).

The graphite also has another effect that derives from its known reaction with the iron during cooling to form the carbide, Fe_3C . Since the molar volume of the carbon in the carbide is smaller than it is in graphite, the carbide's formation during the γ to α transformation is associated with a density increase. This effect is occasionally indicated in the dilatometric record of lower carbon steels as a small negative dilation just following the positive dilation typical of the transformation. More often, however, it is not explicitly indicated at all and is never seen in the dilatometric record of an eutectoid composition such as the present one. The contribution that it makes to the final dimensions of the specimen in such cases is included in

the dilation that accompanies the transformation. An estimate of its magnitude in the present case indicated it to be of the order of -28 μm absolute or about -0.05%.

Not unexpectedly, the dimensional change analysis in this case continued to indicate that the graphite was the dominant factor effecting the behavior of the specimen. As will be evident from the data in Table 3, there were two growth effects listed and including the sintering contribution at 1120 °C, three shrinkage effects. The connections of the graphite to the two growth effects and to the shrinkage at the sintering temperature have already been discussed. The thermal effect and the latent process effects remain. Taken together, these contributed about two thirds of the total shrinkage that the analysis showed.

Significantly, the thermal effect in this case is roughly five times larger than the effect that was indicated for the earlier plain iron specimen, (cf. Table 1). Ostensibly, this difference is very simply due to the difference in the two specimens which, of course, is essentially the admixed graphite. However, to understand what it is that the graphite actually does, recall that the thermal effect is an estimate of the shrinkage that arises as a consequence of the difference in the thermal behaviors of the specimen in the α and γ stability ranges and in addition to the difference in the respective thermal coefficients is otherwise proportional to the differences in the transformation temperatures that are observed during the heating and cooling steps of the process. As reference to the tabulated data of each of the specimens will show, this temperature difference was 97 °C in the present case versus 21 °C in the earlier one. Thus, most of the difference in the indicated thermal effect values is due to this temperature difference which, of course, is directly traceable to the compositional differences of the specimens or, in effect, to the admixed graphite.

Finally, in view of the findings with the latent effects of the earlier specimens, its reasonable to seek a similar explanation of the present effect. However, the earlier procedure of re-sintering the specimen and comparing its behavior to that in the as-sintered condition is not similarly appropriate. The reason is that the specimen now contains the carbide phase and there's no reason to think that its expansion characteristics should be the same as they would be in its absence which, of course, was the case in the as-sintered condition. Instead, its necessary to use the behavior of a plain iron specimen in the re-sintered condition as the standard of comparison. This is admittedly more approximate but its the only possibility. In any case, when this comparison was made, it indicated a relatively modest α phase sintering effect of only -13 μm or -0.024%, leaving an unexplained balance of -2.8 μm or -0.005%. Here again, the influence of the admixed graphite was evident. In the cases of the plain iron specimens, most of the α phase sintering that was indicated occurred at the higher temperatures of the α stability range. In the present case, the sintering was cut short by the onset of the α to γ transformation at a relatively low temperature in the range. Notice, in particular, that this finding correlates with the earlier indication concerning the strength of the sinter bonds that had formed in advance of the transformation.

Sintering Of Iron Powder Plus Graphite Plus Lubricant: F-0008.

The dilatometric results of sintering a compact, again of the same grade iron powder but with admixed graphite and lubricant are shown below in Figure 8 and Table 4.

Sintering of an Iron Powder with Admixed Graphite & Lubricant

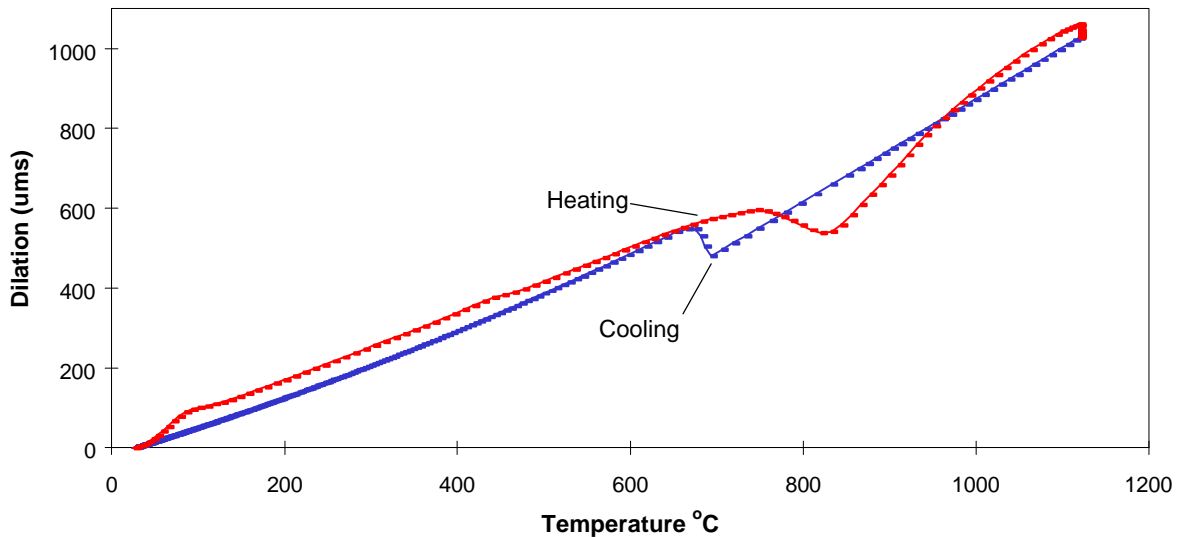


Figure 8 - Dilation vs. Temperature During Sintering of an Iron Powder Compact With Admixed Graphite and Lubricant: F-0008.

Comparison of this figure with the dilatometric record of the iron plus graphite specimen in Figure 7 will show three obvious differences, all of which are traceable to the presence of the admixed lubricant. Of the three, the most important is that the cooling curve in this case intersects the heating curve twice instead of once as in the earlier case and subsequently descends to a near zero dimensional change value. The other differences include the rapid early expansion and the later break in the upward trend of the heating curve above 400 °C. These, of course, are very similar to the effects that were shown by the record of the iron plus lubricant specimen in Figure 5 and have the same explanation.

Interestingly, a more detailed comparison of the present record in Table 4 with that of the iron plus graphite specimen in Table 3 showed only two major differences and one minor one. The major differences were in the details of α to γ transformation and in the values of the latent process effects. The minor one was in the graphite solution effect. As will be discussed, the transformation and graphite solution differences are thought to be related. Otherwise, there was also a large difference in the net contributions that the phase transformations made to the final dimensional change values in each case. However, as may be easily verified by reference to the data, most of this was attributable to the α to γ transformation in the present case and the much larger dilation that accompanied it.

In other respects, the α to γ transformation data in the present case indicated that there was little if any of the sinter bond breaking that is thought to have occurred in the earlier case. The transformation started at 745 °C which is about as low as it's ever seen to start and was accompanied by a dilation of -59.4 µms absolute or -0.110% which is moderately large. These values are obviously in stark contrast with the values of 771 °C and -18.0 µms that characterized the transformation of the earlier specimen. The implication is that the present specimen was well sintered in advance of the transformation and consequently suffered little if any density loss as a result of the stresses that attend the process. On the other hand, this is

not to imply that the stresses had no effect on the dimensions of the specimen since its likely that limited plastic deformation is a frequent if not perennial response to their presence. In particular, it may well be that varying amounts of deformation due to variations in temperature, composition and prior sintering as they effect the yield strength of the specimen are largely responsible for the disparity in the transformation dilations that are generally observed during the heating and cooling steps of the process.

Table 4 - Dilatometric Indications Of The Sintering Of An Iron Power Compact With Admixed Graphite and Lubricant.

Dimensional Change Data		
Condition	ΔL (μms)	$\Delta L/L_0$ %
At 1120 °C	-43.1	-0.080
As-Sintered	-0.5	-0.001
Thermal Data		
Temperature Range °C	Coefficient of Expansion cm/cm/°C	Coefficient of Contraction cm/cm/°C
200 - 400 (α -phase)	1.56E-05	1.51E-05
500 - 650 (α -phase)	1.56E-05	1.62E-05
900 - 1100 (γ -phase)	---	2.33E-05
Transformation Data		
Property	α to γ	γ to α
Start Temperature - °C	745	687
Finish Temperature - °C	825	672
Dilation - (μms)	-59.4	+57.5
Dimensional Change Analysis		
Origin of Contribution	ΔL (μms)	$\Delta L/L_0$ %
Graphite Solution	+150.6	+0.278
Thermal Effects	-115.0	-0.212
Net Transformation Dilation	-1.9	-0.004
Latent Process Effects	+8.9	+0.016

The α to γ transformation data also showed that the transformation finish temperature of the present specimen was higher than that of the earlier specimen by 20 to 25 °C. Interestingly, its likely that the growth that's attributable to the dissolution of the graphite that still remains to go into solution after the transformation is largely determined by the finish temperature. For example, the transformation finish temperature of the earlier specimen was 803 °C which according to the Fe-C binary diagram corresponds to an equilibrium carbon content of ~0.3%. Thus, there was about 0.5% graphite remaining to go into solution after the transformation. In contrast, the finish temperature of the present specimen was 825 °C which corresponds to an equilibrium carbon of ~0.22% and indicates that the undissolved graphite content in this case was ~0.58%. This is roughly 15% greater than the earlier value. Thus, the observed growth due to graphite solution in this case would be expected to be similarly greater. In fact, as reference to the tabulated data in the two cases will confirm, it was just upwards of 11% greater. More generally, it will be evident that higher α to γ transformation finish temperatures will normally result in larger graphite solution effects.

The indications of the dimensional change analysis of this specimen including especially, the latent process contribution, were particularly interesting because while they ultimately confirmed the expectation of significant α phase sintering, they did so in a somewhat circuitous manner. To begin with, notice that according to the data in Table 4, the final growth of the specimen was mostly attributable to the graphite solution effect and that the combined contributions of the sintering effect at 1120 °C and the thermal effect which the data indicated were more than sufficient to offset it. Although comparatively small, the net transformation dilation also opposed it. Consequently, the latent process effects in this case turned out to have a positive value and thus indicated either the existence of an additional growth effect that had yet to be considered or experimental error. In either case, given the earlier strong evidences of the likelihood of significant sintering in advance of the α to γ transformation, this was an unexpected finding.

As to the possibility of an additional growth effect, the early rapid expansion associated with the presence of the lubricant was an obvious candidate. To examine this possibility, precisely the same comparison to re-sintered plain iron as was previously explained as being needed to show the presence of an α phase sintering effect in the iron plus graphite specimen was needed here as well. This comparison is shown below in Figure 9.

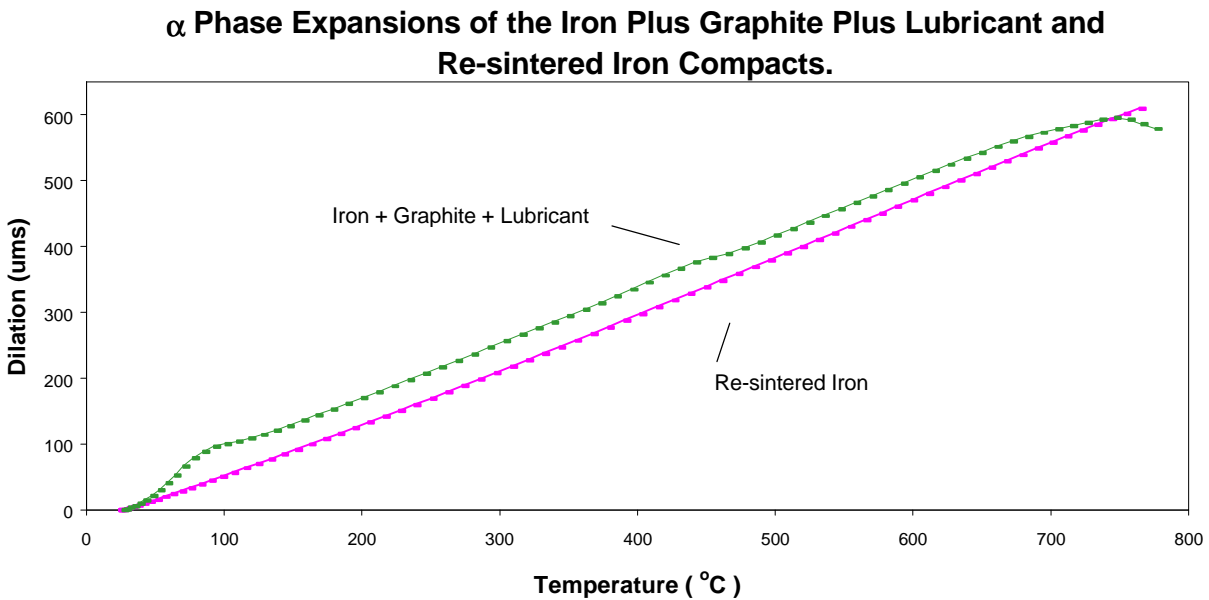


Figure 9 - α Phase Expansion of an Iron Plus Graphite Plus Lubricant Specimen versus a Re-sintered Plain Iron Specimen

Interestingly, what the curves in this figure showed was that the anticipated α phase sintering actually did occur but was only just sufficient to offset what remained of the early rapid expansion of the lubricant after the contraction which accompanied its decomposition at a higher temperature. As a consequence, the findings in the figure did not really appear to explain the observed latent effects value. As it turned out, the underlying hard data both confirmed this and showed that the magnitude of the indicated sintering effect was about -32.4 ums absolute or -0.060%. Significantly, this was nearly three times the magnitude of the α

phase sintering effect that the same comparison showed in the earlier iron plus graphite specimen. As regards the latent effects value, it was subsequently concluded that in this instance, it was largely due to experimental error. For example, either an under-estimate of the graphite solution effect or an over-estimate of the thermal effect could easily account for most, if not all of it.

In any case, given that the admixed lubricant represented the essential compositional difference between this and the previous specimen, it once again appeared that its presence had had a profound effect on the amount of sintering that occurred especially, in the α stability range.

.Sintering Of Iron Powder Plus Graphite Plus Copper Plus Lubricant: FC-0208.

The dilatometric results of sintering a compact, again of the same grade iron powder but with admixed graphite, copper and lubricant are shown below in Figure 10 and Table 5.

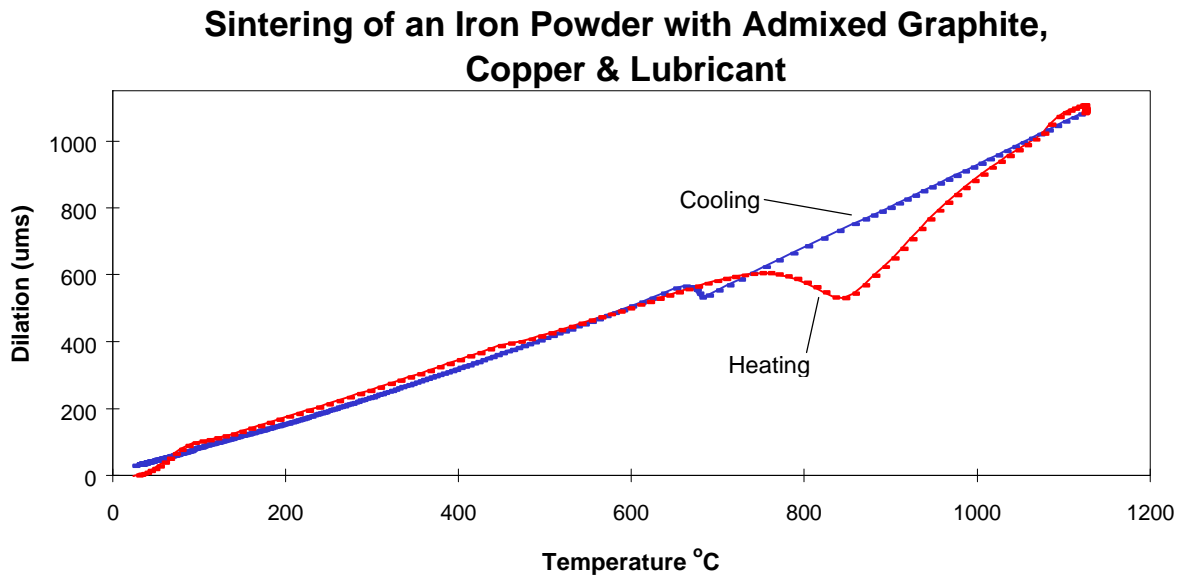


Figure 10 - Dilation vs. Temperature During Sintering of an Iron Powder Compact With Admixed Graphite, Copper and Lubricant: F-0208.

Comparison of this figure with the dilatometric record of the previous specimen in Figure 8 will show only two obvious differences, both of which are traceable to the presence of the copper. One is that the cooling curve in this case intersects the heating curve five times instead of twice as in the earlier case and subsequently descends above it to indicate a small net growth. The other is a rapid expansion in the heating curve just before the maxima at 1120 °C. As explained below, this was apparently due to the melting of the copper and the appearance of a liquid phase.

In contrast to the indications of the figures, reference to the tabulated data of the two specimens will show that except for the thermal coefficients, there were significant differences in just about every other property listed. These are separately reviewed and discussed below.

In spite of the presence of the liquid phase or, as will be explained, almost certainly because of it, the shrinkage at the sintering temperature in this case was only about 50% of the value that was observed in the earlier specimen, (e.g. -23 ums vs -43 ums). Significantly, although the presence of a liquid phase will usually have a beneficial sintering effect in terms of metallurgical bonding and pore rounding, it doesn't always result in shrinkage and may, in fact, have exactly the opposite effect. Precisely what it does is largely dependent on its wetting properties, its phase relations with the base powder and the volume fraction present.

Table 5 - Dilatometric Indications Of The Sintering Of An Iron Power Compact With Admixed Graphite, Copper and Lubricant.

Dimensional Change Data		
Condition	ΔL (ums)	$\Delta L/L_o$ %
At 1120 °C	-22.7	-0.042
As-Sintered	+30.9	+0.057
Thermal Data		
Temperature Range °C	Coefficient of Expansion cm/cm/°C	Coefficient of Contraction cm/cm/°C
200 - 400 (α -phase)	1.59E-05	1.53E-05
500 - 650 (α -phase)	1.52E-05	1.68E-05
900 - 1100 (γ -phase)	- - -	2.34E-05
Transformation Data		
Property	α to γ	γ to α
Start Temperature - °C	755	681
Finish Temperature - °C	841	662
Dilation - (ums)	-77.6	35
Dimensional Change Analysis		
Origin of Contribution	ΔL (ums)	$\Delta L/L_o$ %
Graphite & Copper Solution	+197.2	+0.364
Copper Melting	+30.0	+0.055
Thermal Effects	-123.5	-0.228
Net Transformation Dilatation	-42.6	-0.079
Latent Process Effects	-7.5	-0.014

In the case of copper in an FC-0208 composition, none of these factors favor shrinkage. For example, the dihedral angle of the copper at this carbon content is reportedly in excess of 35°, (7). As a consequence, it can only penetrate the grain boundaries at their intersections, (e.g. at triple points), and combined with its poor solubility for iron will typically provide little if any shrinkage by grain boundary transport, (8). On the other hand, basically the same wetting properties also dictate that it otherwise spread into the finest pores and thus, as the liquid appears, it promptly increases its surface area of contact with the iron. Then owing to its solubility in the iron and the fact that it diffuses faster in the iron than visa versa, it quickly goes into solution and displaces most if not all of its volume and, like graphite, produces a growth effect, (9). Of course, copper will also cause growth in the solid state as well but obviously, owing to its wetting effects as a liquid, would be expected to do so much faster once it melts.

As the data in the tables further show, the α to γ transformation in this case started and finished at somewhat higher temperatures and was accompanied by a substantially larger dilation than earlier, (e.g. -78 μms vs -59 μms). Conversely, the γ to α transformation now started and finished at lower temperatures and was accompanied by a substantially smaller dilation than previously, (e.g. +35 μms vs +57 μms). The higher transformation temperatures in the first instance may indicate a tendency of the copper to impede graphite solution by virtue of the effect it has in increasing the thermodynamic activity of carbon in iron, (10). The lower start temperature of the cooling transformation on the other hand is almost certainly due to an inhibiting effect of the copper on α phase nucleation as is typical of virtually every other first transition series alloy addition, (11). For various reasons as already discussed, the origin of the observed transformation dilation differences between the two specimens is uncertain. However, the resulting net transformation dilation value in the present case more than made up for the aforementioned decreased sintering effect.

As indicated in Table 5, the γ phase expansion after the transformation in this case but in advance of the appearance of the liquid phase apparently included both graphite and copper solution effects. For example, the curvature of the heating curve up to but not including the rapid expansion indicated a growth value that, as shown in the table, was nearly 25% larger than the graphite solution value of the previous specimen. However, only a part of this increase was explainable by the above increase in the α to γ transformation finish temperature as being due to an increase in the residual graphite content of the specimen after the transformation. Thus, the balance was attributable to copper that went into solution from the solid state.

The reason why the rapid expansion in the heating curve just before the specimen attained the sintering temperature was thought to be correlated with the appearance of the liquid phase was because it started at roughly the melting point of copper and then leveled off again just above the peritectic temperature as indicated in the Cu-Fe binary diagram, (12). As shown in Table 5, the associated growth effect was +30 μms absolute or 0.055%. The growth per se is thought to be attributable to plastic deformation of the compact in response to the density decrease that accompanies the melting of the copper. Presumably, as the copper melts it expands and particles that were initially encapsulated by the iron during the compaction step stress the surrounding matrix and deform it. The usual explanation that the growth is a consequence of the newly formed liquid penetrating the grain boundaries doesn't appear to make sense here because, as earlier explained, what's known about the liquid's wetting properties indicates that its action in this respect is limited to the grain boundary intersections which, of course, can have no effect on the compact's dimensions.

The thermal effects value that was indicated in this case was also slightly larger than in the previous specimen and reflects the modest differential in the heating and cooling transformation temperatures that was earlier indicated.

Finally, in spite of all of the foregoing differences, the dimensional change analysis in this case gave a similar result to that of the previous specimen. The latent process effects value that was indicated was negative instead of positive but was again fairly small. Significantly, the heating curve of the present specimen in advance of the α to γ transformation was virtually identical to that of the previous specimen. Thus, a similar analysis in search of an α phase sintering effect gave essentially the same result as previously, (i.e. ~32 μms absolute or -

0.060%), as well as indicating that the present latent effects value was likewise due to experimental error.

SUMMARY AND CONCLUSIONS

The objective of the present paper was to call attention to the fact that the dimensional changes of the most common P/M compositions, namely F-0008 and FC-0208, are largely determined by processes and effects that occur during the heating and cooling stages of the sintering process rather than at the sintering temperature. The dilatometric records of a series of sintering trials that started with a pure grade of iron powder and progressed in compositional increments to the FC-0208 composition were presented and discussed in support of this contention.

The sintering of a plain iron powder specimen indicated a final dimensional change of -0.19%. Of this, only about 3% was attributable to shrinkage that occurred at the sintering temperature. The balance was due to transformation effects and α phase sintering. The transformation effects included net dilation and thermal effects values that accounted for upwards of 55% of the indicated change. The net dilation value is the sum of the shrinkage and growth effects that accompany the forward and reverse transformations during the heating and cooling stages of the process. It derives basically from the different densities of the α and γ phases but is ultimately determined by several factors including especially the sintering that precedes the transformations and the stress states that accompany them. The thermal effects value arises as a result of the differing thermal characteristics of the phases and the differences in the transformation temperatures. The α phase sintering contribution mentioned accounted for the remainder of the change or about 41%. It was detected by reference to the sintering behavior of the specimen in the re-sintered condition.

The sintering of an iron plus lubricant specimen indicated a final dimensional change of -0.33%. Of this, only about 4% was attributable to shrinkage that occurred at the sintering temperature. The balance was again due to transformation effects and α phase sintering. However, in this case, their relative contributions were essentially reversed with just a little less than 55% of the change now being attributable to sintering in the low temperature regime and the remainder to the net dilation and thermal effects values. There were also several interesting lubricant effects including a low temperature expansion and a later contraction that attended its decomposition at $\sim 450^\circ\text{C}$. These effects were later shown by reference to the specimen in the re-sintered condition to be offsetting and thus to have had no net effect on the final dimensional change value. On the other hand, it was also evident by comparison of the α phase sintering contribution in this case to that of the earlier specimen that the lubricant had apparently had some sort of an activating effect. Subsequent limited studies to explain it, however, were unsuccessful.

The sintering of an iron plus graphite specimen indicated a final dimensional change of +0.12%.

Interestingly, the shrinkage that occurred at the sintering temperature in this case was about two thirds of this value and was therefore substantially larger than either of those of the earlier sinterings. The increase was attributed to an effect of dissolved carbon in increasing the diffusivity of iron. More generally, there were five other effects that also made contributions to the final result. Each was directly or indirectly traceable to the presence of the graphite. The largest growth effect was attributed to graphite solution subsequent to the α to γ transformation. Instead of indicating shrinkage as in the earlier findings, the net transformation

dilation in this case added a further increment of growth. The dilatometric record indicated that this was largely a consequence of a relative density loss during the α to γ transformation due to limited α phase sintering in advance of the change and the resultant inability of the pre-existing sinter bonds to survive the stresses that accompanied it. On the other hand, it was noted that although not explicitly indicated in the data, the known formation of Fe_3C during the later γ to α transformation was associated with a modest density increase and had to be counted as being a beneficial effect of the graphite. Otherwise, the largest explicit shrinkage in the data was the thermal effects value. This too was regarded as a beneficial effect of the graphite in increasing the temperature differential between the heating and cooling transformations. Finally, the earlier hints of limited sintering in advance of the α to γ transformation were confirmed. The indications were that the relatively early onset of the α to γ transformation due to the graphite had reduced the α phase sintering in this case to a small fraction of the values that were earlier observed. Owing to the presence of the carbide in the final sintered condition of this specimen, the latter effect was shown by reference to the sintering behavior of an earlier plain iron specimen in the re-sintered condition.

The sintering of the iron plus graphite plus lubricant specimen, (i.e. the F-0008 composition), indicated a final dimensional change value of zero. Here again, there was a large shrinkage at the sintering temperature which taken by itself appeared to be unrelated to the latter finding. Not unexpectedly, the value of this shrinkage was essentially equal to that of the previous specimen and direct comparison of the dilatometric records of the two otherwise showed that the difference in their final dimensional change values was largely attributable to two differences in their respective sintering behaviors. One had to do with the amount of α phase sintering that preceded the α to γ transformation and the other was in the details of the transformation itself. Using identically the same comparison to re-sintered iron as previously, the indication as to the amount of α phase sintering in this case was that it had been nearly three times as large as in the previous specimen. In view of the earlier findings relative to the effect of the lubricant in activating α phase sintering in the plain iron specimen, it was speculated that the present difference was likewise attributable to the same cause. In any case, presumably as a consequence, the transformation data in this case presented little or no evidence of the relative density losses that were earlier indicated. The transformation started at a lower temperature, finished at a higher one and most importantly, was accompanied by a shrinkage that was roughly four times larger than in the previous specimen. The upshot was that the net transformation dilation now indicated shrinkage rather than growth as earlier and the resultant thermal effects value which always indicates shrinkage was nearly twice what it had been in the previous specimen. As a matter of additional interest, this specimen also indicated a minor increase in the growth attributable to graphite solution during the heating step which was shown by reference to the Fe-C binary diagram to be correlated with the aforesaid increase in α to γ transformation finish temperature.

The sintering of an iron base specimen with admixed graphite, copper and lubricant, (i.e. the FC-0208 composition), indicated a final dimensional change of +0.06%. As previously, this finding was again contra-indicated by the occurrence of a net negative change at the sintering temperature. However, this shrinkage was only about half that seen in the previous F-0008 specimen indicating that the presence of the copper had been associated with growth due to solution effects rather than shrinkage due to liquid phase sintering. More generally, comparison of the dilatometric records of these specimens showed that the difference in their final change values was largely attributable to four additional differences which were likewise all traceable to the copper. The first and largest of these was manifest as a rapid expansion in

the heating curve that was correlated with the initial appearance of the liquid phase. It was speculated to be a deformation effect of the copper due to the expansion that attends the density decrease it undergoes upon melting. The second difference was in the growth indicated by the heating curve in advance of the rapid expansion event. This was about 25% greater than that of the

F-0008 specimen and thus was thought to indicate copper solution from the solid state in addition to growth due to graphite solution effects. The remaining differences included an increase in the temperature range of the α to γ transformation and a decrease in the start temperature of the reverse transformation. Contrary to the foregoing, these differences were ultimately associated with shrinkage rather than growth. The first was thought to reflect a known thermodynamic tendency of copper to reduce the affinity of carbon for iron whereas the second was evidently due to an ordinary alloy effect on hardenability. The important contribution of the lubricant in promoting sintering in advance of the α to γ transformation was apparently unaffected by the presence of the copper in so far as the observed effect in this case was of the same magnitude as in the F-0008 specimen.

Finally, as a general matter, it will be evident that dilatometry is a powerful analytical technique which has considerable potential to reveal the intricacies of the sintering process. Notice also, however, that it is neither a simple method nor a very expeditious one. More specifically, the average study is lengthy and may raise more questions than it answers. For example, the present study clearly showed the existence of a beneficial effect of the lubricant on sintering but otherwise failed to explain it. Thus, if the study had originally been undertaken, for example, to mitigate some adverse effect in the sintering of the FC-0208 composition, then in spite of all that's been done to this point, it would still only be partially complete. Indeed, it could very well be that it would be no better than in its very earliest stages. Consequently, it will be appreciated the while dilatometry has significant potential relative to understanding sintering, its essentially a research tool and not generally applicable to solve the day to day problems that are typically encountered with the process.

ACKNOWLEDGMENTS

Special thanks are due to Mr. W. R. Bentcliff of this laboratory for his many useful suggestions and his help in specimen preparation and testing.

REFERENCES

1. H. E. Exner, "Principles of Single Phase Sintering", *Rev. Powder Met. Phys. Ceram.* 1979, Vol. 1, pp 16-19.
2. J. Askill, "Tracer Diffusion Data for Metals, Alloys, and Simple Oxides", Plenum Data Corp., New York, 1970, pp 34.
3. W. Schatt, E. Friedrich, and K. P. Wieters, "Dislocation Activated Sintering", *Rev. Powder Met. Phys. Ceram.* 1986, Vol. 3, pp 1-111.
4. D. Saha, and D. Apelian, "Optimization of De-Lubrication During Sintering", Metal Processing Institute, WPI, Worcester, MA., 2000.
5. M. Hansen, "Constitution of Binary Alloys", Mcgraw-Hill Book Co. New York, 2nd Ed., 1958, pp 353-365.
6. J. Askill, *Ibid* pp 63.

7. R. L. Lawcock, and T. J. Davies, "Effect of Carbon on Dimensional and Microstructural Characteristics of Fe-Cu Compacts During Sintering", *Powder Metallurgy*, Vol. 33, No. 2, Pergamon Press, New York, NY, 1990, pp 147-150.
8. P. J. Wray, "The Geometry of Two-Phase Aggregates in Which the Shape of the Second Phase Is Determined By Its Dihedral Angle", *Acta Metallurgica*, Vol. 24, Pergamon Press, New York, NY, 1976, pp 125-135.
9. Y. Trudel, and R. Angers, "Comparative Study of Fe-Cu-C Alloys Made From Mixed and Prealloyed Powders", *Modern Developments in Powder Metallurgy - 1974*, Vol. 6, pp 305, Metal Powder Industries Federation, Princeton, NJ.
10. R. Williams, and C. Bodsworth, "Effect of Cobalt, Copper, and Manganese on the Thermodynamic Activity of Carbon in Iron-Base Austenites", *JISI*, Feb., 1972, pp 106-110.
11. E. C. Bain, and H. W. Paxton, "Alloying Elements in Steel", 2nd Ed. ASM Metals Park, OH, 1961, pp 123-181.
12. M. Hansen, *Ibid*, pp 580-582.